Reaction Invariance and Stability in Catalyst Particles for Production of Methanol

Odd Andreas Asbjornsen
Dept. of Thermal Energy and Hydro Power, Norwegian University of Science and Technology, N-7034
Trondheim-NTH, Norway

Magne Hillestad
Statoil a.s., Corporate Research Center, Ranheimsveien 10, N-7005 Trondheim, Norway

Industrial practice requires immediate and adequate responses to simple questions asked. For example, does a catalyst particle show any tendency to thermal oscillations in the form of a limit cycle? The root to such cycles is found in the eigenvalues of the Jacobian matrix to the reaction rate vector, applying the concept of reaction invariance, a direct consequence of Avogadro's stoichiometric principle for homogeneous stirred tank reactors. However, this concept does not generally apply to heterogeneous reactor dynamics, because it is found in the heterogeneous transports of heat, reactants and products. The transport is an irreversible phenomenon that usually contributes to shifting the eigenvalues to the left and hence increases the stability. Still, effects of transport mechanisms, both internally and externally, on the catalyst particle are important to assess in such industrial analyses. A practical industrial reactor for methanol production was the subject for stability studies, which concluded that thermal oscillations are not likely to occur. During this study, a number of interesting details were examined such as rank deficiency of the reaction matrix and root loci for the temperature dependence of the Jacobian matrix eigenvalues. A practical consequence of eventual thermal cycling of the catalyst particles is a long-term degradation of the catalyst efficiency, as seen in the ammonia synthesis.

Introduction

Conservation and balance are different principles for chemical processes; they cover different properties and give different results. The basic difference between conservation and balance is found in the production and consumption terms. For example, mass is conserved and species are balanced; energy is conserved with energy forms (such as heat) balanced. In reaction engineering, the Avogadro stoichiometric principle is generally accepted as the conservation principle, which applies to atoms in the reaction schemes (Glasstone and Lewis, 1964; Aris, 1969; Asbjornsen and Fjeld, 1970; Asbjornsen, 1972, 1987a,b; Fjeld et al., 1974) and to electrical charge in the electroneutrality principle (Lewis and Randall, 1961; Asbjornsen, 1987c). They become invariant to the way reactions proceed.

Using the concepts of reaction invariance, it is well-known (Aris, 1969; Asbjornsen and Fjeld, 1970; Asbjornsen, 1972, 1987a,b, 1992; Fjeld et al., 1974) that the stability of an adiabatic stirred tank reactor is determined by the eigenvalues of the Jacobian matrix J to the reaction rate expression and the stoichiometric matrix

$$J = \left[\frac{\partial r}{\partial c} N + \frac{\partial r}{\partial T} \Delta T_{ad}^{T} - \sigma I \right] \tag{1}$$

Here is r the reaction rate vector ($\text{mol}\cdot\text{kg}^{-1}\cdot\text{s}^{-1}$), N the transpose of the stoichiometric matrix and ΔT_{ad} the adiabatic temperature rise of the reactions ($\text{K}\cdot\text{kg}\cdot\text{mol}^{-1}$). Superscript T is defined as a transpose. If the reaction matrix J has eigenvalues in the right half plane, the reaction itself may exhibit runaway conditions. In industrial practice, it is important to identify such conditions as early as possible in the process design. Indeed, the clarification of the stability conditions of catalyst particle of the methanol reactor is the main emphasis of this research.

The eigenvalues λ_j of the reaction matrix $\boldsymbol{J}$ in Eq. 1 are shifted to the left (Asbjornsen, 1974) by the space velocity, σ. Those very simple and general results are based on the application of the fact that the atom conservation is reaction invariant, which simplifies the order of the eigenvalue problem to the number of reactions provided the stoichiometric matrix has full rank. In the methanol synthesis, the stoichiometric matrix does not have full rank. The stoichiometry of one reaction is a linear combination of those of the other reactions. However, the eigenvalue problem of the reaction reduces to the number of reactions with linearly independent stoichiometry, as one may write all reaction rates as linear combinations of a basic rate vector $\boldsymbol{r}''$

$$\boldsymbol{r} = \boldsymbol{R}''\boldsymbol{r}'' \tag{2}$$

The Jacobian in Eq. 1 is modified and reduced accordingly

$$\boldsymbol{J} = \left[\left\{\frac{\partial \boldsymbol{r}''}{\partial \boldsymbol{c}}\boldsymbol{N} + \frac{\partial \boldsymbol{r}''}{\partial T}\Delta \boldsymbol{T}_{ad}^{T}\right\}\boldsymbol{R}'' - \sigma \boldsymbol{I}\right] \tag{3}$$

This modification indeed applies to the methanol synthesis, as shown later in this article.

Purpose of Investigation

It has been observed in the industrial practice (such as in the ammonia synthesis) that the catalyst temperature may oscillate during operation. The operating conditions in this region give rise to this behavior, which is seen as oscillations in the temperature from a temperature sensor in the vicinity of the unstable region. What is then observed is an unstable operating condition of catalyst particles giving rise to limit cycles through extinction and ignition of the particles. The temperature fluctuations are harmful to the catalyst and reduce its lifetime. Limit cycles of this nature were reported by Hugo (1971) for the oxidation of carbon monoxide. He was concerned with the dynamic behavior of a laboratory reactor and not the catalyst particle *per se*. However, it may become evident that the stability problem stems from the catalyst particles themselves. A careful study of some dynamic characteristics of one single catalyst particle seems worthwhile.

The stability study of the methanol reactor has many aspects starting in a bottom up fashion from the catalyst particle to the overall stability of the heat recovery cycle. The purpose of this investigation is to examine the stability conditions for the catalyst particle under normal operating temperature profiles through the reactor under construction. If stability is not assured at the catalyst particle level, there are few degrees of freedom to mitigate the problem once the operating temperature profile is established. The important processes to consider are the transfer of heat and chemical species, the reaction kinetics, and the heat and mass accumulation properties of the pellet. If the reaction matrix is stable for all operating conditions, the transport phenomena are known to improve the stability, as commented above.

Reaction Invariant States

The molecular atomic matrix A (Asbjornsen, 1987b, 1992) and the stoichiometric matrix N are orthogonal, which means that $\boldsymbol{AN} = \boldsymbol{O}$. The simple reaction invariance principle for stirred tanks and tubular reactors (Asbjornsen, 1972, 1987b, 1992; Fjeld et al., 1974) only applies if the species are transported through the reactor by convection, not by diffusion or conduction, as is the case for a catalyst particle. This is due to the different transport phenomena for the species. However, such irreversible transport processes contribute to increased stability of the reaction system. A stable subsystem related to the transports is driven by the reactions. This may be visualized by a decomposition of the concentration vector

$$\boldsymbol{c} = \boldsymbol{A}^{T}\boldsymbol{x} + \boldsymbol{N}\boldsymbol{h} \tag{4}$$

Here is A the atomic matrix, N the stoichiometric matrix, $\boldsymbol{x}$ a vector equivalent to the concentration of atoms (atom kg^{-1}), and $\boldsymbol{h}$ equivalent to the extent of reactions ($\text{mol}\cdot\text{kg}^{-1}$). $\boldsymbol{c}$ is the component concentration vector ($\text{mol}\cdot\text{kg}^{-1}$). Then, premultiplying Eq. 4 by $\boldsymbol{A}$, gives the concentration of atoms at any time

$$\boldsymbol{x} = [\boldsymbol{A}\boldsymbol{A}^{T}]^{-1}\boldsymbol{A}\boldsymbol{c} \tag{5}$$

and the extent of reactions at any time ($\text{mol}\cdot\text{kg}^{-1}$)

$$\boldsymbol{h} = [\boldsymbol{N}^{T}\boldsymbol{N}]^{-1}\boldsymbol{N}^{T}\boldsymbol{c} \tag{6}$$

The general mass balance with the transport phenomena is now combined with the heat balance at the catalyst temperature T (K). A new state vector y ($\text{mol}\cdot\text{mol}^{-1}$) is expanded by the temperature T the atomic matrix, A is expanded by the heat of formation of the components ($-\Delta \boldsymbol{H}_f$) ($\text{J}\cdot\text{mol}^{-1}$) and into a new matrix $\boldsymbol{E}$, the heat of reactions ($-\Delta \boldsymbol{H}_r$) ($\text{J}\cdot\text{mol}^{-1}$) are included in a new stoichiometric matrix $\boldsymbol{B}$ which is modified by the catalytic activity and the adiabatic temperature rise by the catalyst as follows:

The augmented state vector includes T

$$z = \begin{bmatrix} c \\ T \end{bmatrix} \tag{7a}$$

This leads to an augmented stoichiometric matrix

$$\boldsymbol{B} = \begin{bmatrix} N \\ \Delta T_{ad}^{T} \end{bmatrix} \tag{7b}$$

Which again leads to a similarly augmented atomic matrix

$$\boldsymbol{E} = \begin{bmatrix} A & 0 \\ -\Delta T_f^{T} & 1 \end{bmatrix} \tag{7c}$$

Here are ΔT_{ad} and ΔT_f, the adiabatic temperature rise due to the heats of reaction and formation, respectively ($\text{K}\cdot\text{kg}\cdot\text{mol}^{-1}$). They are defined as

$$\Delta T_{ad} = \frac{-\Delta H_r}{\epsilon \rho c_p} \text{ and } \Delta T_f = \frac{-\Delta H_f}{\epsilon \rho c_p} \tag{7d}$$

The average heat capacity by volume $\epsilon \rho c_p$ is defined by Eq. 13 later. ρ is density ($\text{kg} \cdot \text{m}^{-3}$).

Properties of Heat of Formation and Heat of Reaction

According to the thermodynamic fundamentals of chemical reactions (Denbigh, 1964), the following enthalpy relation is always satisfied by the heats of formation and the heats of reaction

$$\left(-\Delta H_f^T\right) N - \left(-\Delta H_r^T\right) = 0^T \tag{8}$$

Therefore, the two matrices B and E are orthogonal

$$EB = O \tag{9}$$

Those results are based on a simple decomposition of the reactor state space into a reaction invariant subspace, orthogonal to the reaction rate subspace. This is indeed convenient in reactor modeling and simulation, and in reactor experiments. In modeling, the fact that the reactor state space may be decomposed into two orthogonal subspaces simplifies the model and reduces the mathematical and numerical complexity. In experimentation, the reaction invariant subspace makes it possible to isolate purely physical phenomena (such as residence time distributions) (Asbjornsen, 1960, 1962, 1987, 1989) while reactions are actually proceeding.

Catalyst Pellet

The catalyst pellet is the crucial element in catalytic reactor systems. Transport phenomena are as important as the catalytic properties in evaluating the efficiency and selectivity of a catalytic reactor. Consequently, the packed catalyst reactor bed has been the subject of a large number of theoretical and experimental investigations (Aris, 1969; Hugo, 1971; Wicke et al., 1971; Balakotaiah and Luss, 1991; Philippou et al., 1993). The emphasis in the work of those researchers has been put on the steady-state multiplicity of catalytic reactors, and the operating conditions where such multiplicity may occur. The studies are extended to steady-state multiplicity of catalyst pellets by Hu et al. (1986). Few studies have been related to a practical problem addressed here, namely, the reaction invariance and dynamic stability of a single catalyst pellet in an industrial reactor under the operating conditions dictated by the concentration and temperature profiles along the catalytic reactor itself.

The catalyst pellet (Figure 1), which is porous, has a large area per unit mass of the pellet. Therefore, the pellet has a certain capacity to accumulate heat and components participating in the reaction. The controlling mechanism for the transfer processes are the boundary layers around the pellet and the eventual transport mechanisms within the porous pellet. The exothermic reactions take place at the pellet surface, where the heat- and mass-transfer processes occur. In the beginning, it is advised to not complicate the model too much. Hence, simplifying, but rational assumptions are usually proposed. Such assumptions, which later are relaxed, are the following:

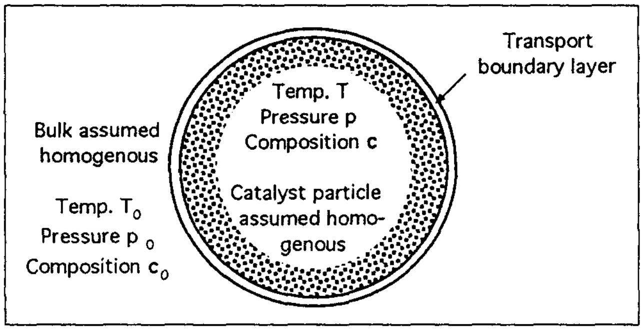

Figure 1. Catalyst pellet with heat and mass transfer.

- Temperature and surface concentration gradients within the pellet are ignored.
- Transport properties are assigned to the total catalyst contact surface only, that is, the interface between gas and solid throughout the catalyst.
- The shape of the catalyst particle is spherical.

With those assumptions, it is possible to interpret the conditions for possible oscillations on a purely physical basis. Due to the time lag between heat flux, heat accumulation and reaction heats, oscillations may occur if heat flux and heat released by reaction are out of phase. The controlling parameters here are the eigenvalues of the catalyst pellet dynamics. A mathematical model is required to study those aspects in more detail.

Mathematical Model of Catalyst Pellet

A single catalyst pellet is taken as a functional unit. Such a particle has a weight W_c in kg and a surface contact area of A_c in m^2. The accumulation capacities are characterized by a specific heat capacity c_{pc} in $\text{J} \cdot \text{kg}^{-1} \cdot \text{K}^{-1}$, and a gas accumulation volume of V_a in m^3. The gas composition c in mole m^{-3} is most uniquely defined on a volume basis for dynamic simulations where the pellet volume is constant. The reaction rates $r(T, c)$ in $\text{mol} \cdot \text{kg}^{-1} \cdot \text{s}^{-1}$ may be specified as intensive properties per unit mass of the catalyst, being a function of temperature and surface concentration of the various components. The reaction mechanisms are characterized by the dimensionless stoichiometric matrix N, and the molecular formulae by a dimensionless atomic matrix A. The coefficients ν_i in the matrix N are positive for products being produced and negative for reactants being consumed. The coefficients are 0 for inert components and for components not participating in a reaction. The specific heats of reaction are collected in a vector $(-\Delta H)_r$ in $\text{J} \cdot \text{mol}^{-1}$, and the heats of formation of components are grouped in the vector $(-\Delta H)_f$, also in $\text{J} \cdot \text{mol}^{-1}$. The state of the bulk of the gas outside the catalyst pellet is given index o. The surface reaction rate is defined at constant pressure

On a catalyst mass basis: $r' = r'(c, T)$ (10a)

On a catalyst volume basis, as used here: $r = \rho_p r'(c, T)$ (10b)

The transport phenomena across the boundary layer are simplified by transfer coefficients, by the first assumption assumed to be mutually independent or uncorrelated. There is a driving potential to the catalyst pellet for reactants and from the catalyst pellet for products. Hence, we may deal generally with component transport as well as with total mass transport. The mass-transfer coefficients are grouped into a diagonal mass-transfer coefficient matrix $\boldsymbol{K}$ in $\mathrm{kg \cdot m^{-2} \cdot s^{-1}}$. In the simplest case, the flux of all components is expressed by a component flux vector $\boldsymbol{n}$, in $\mathrm{mol \cdot m^{-2} \cdot s^{-1}}$

$$\boldsymbol{n} = \boldsymbol{K}(\boldsymbol{c}_o - \boldsymbol{c}) \tag{11}$$

This equation is augmented by the heat transport q in $\mathrm{W \cdot m^{-2}}$

$$\begin{bmatrix} \boldsymbol{n} \\ q \end{bmatrix} = \begin{bmatrix} \boldsymbol{K} & \boldsymbol{0} \\ \boldsymbol{0}^T & h \end{bmatrix} \begin{bmatrix} c_0 - c \\ T_0 - T \end{bmatrix} \tag{12}$$

Subscript 0 is bulk gas conditions. F is the general heat-transfer coefficient. For simplicity in the stability analysis of the particle in an industrial reactor, Eqs. 12 and 8 are used for the catalyst stability analysis. The component mass balances are then very simple, once the catalyst particle is regarded as a simple "stirred tank." The heat balance is equally simple, when the average heat capacity for the solid particle and the gas is used as

$$\rho c_p = \frac{1-\epsilon}{\epsilon} \rho_p c_{p,p} + \rho_g c_{p,g} \tag{13}$$

$$\frac{d}{dt}\begin{bmatrix} c \\ T \end{bmatrix} = \frac{6}{\epsilon d_p} \begin{bmatrix} \boldsymbol{K} & \boldsymbol{0} \\ \boldsymbol{0}^T & h/\rho c_p \end{bmatrix} \begin{bmatrix} c_0 - c \\ T_0 - T \end{bmatrix} + \mathbf{Br} \tag{14}$$

Here ϵ is the porosity of the catalyst, and the ratio $6/d_p$ ($\mathrm{m^{-1}}$) is the surface area per unit volume of the catalyst. h is the general heat-transfer coefficient ($\mathrm{W \cdot m^{-2} \cdot K^{-1}}$). The adiabatic temperature rise $\Delta \boldsymbol{T}_{ad}$ for the catalyst particle is (Aris, 1967) $\Delta \boldsymbol{T}_{ad} = (-\Delta \boldsymbol{H})^T / (\rho c_p)$.

The augmented transport coefficient matrix (including heat transfer) is $\boldsymbol{T}$, and the augmented state vector is $\boldsymbol{z}$. The complete model for the catalyst particle, provided the above assumptions hold, is then

$$\frac{dz}{dt} = \boldsymbol{T}(z_0 - z) + \boldsymbol{B}\boldsymbol{r} \tag{15}$$

The augmented state vector may again be decomposed into two orthogonal subsets, such that two orthogonal subspaces appear

$$z = \boldsymbol{E}^T \xi + \boldsymbol{B}\eta \tag{16}$$

From a premultiplication with $\boldsymbol{E}$ and $\boldsymbol{B}^T$, respectively, it may be seen that the following relations are satisfied if the matrices $\boldsymbol{B}$ and $\boldsymbol{E}$ have full rank. This may not be true, as shown by the methanol synthesis reaction below. With the full rank of $\boldsymbol{B}$ and $\boldsymbol{E}$, their pseudoinverse exist (Åström and Wittenmark, 1984)

$$\xi = [\boldsymbol{E}\boldsymbol{E}^T]^{-1} \boldsymbol{E} z \tag{17}$$

and

$$\eta = [\boldsymbol{B}^T \boldsymbol{B}]^{-1} \boldsymbol{B}^T z \tag{18}$$

η is the augmented extent of reaction vector, including heat, and ξ is the augmented reaction invariant vector, including heat.

Effects of Transport Properties

In an attempt to decompose the total dynamic model for the catalyst particle, Eq. 15, the decomposed state is introduced and the equation is premultiplied by $\boldsymbol{E}$ and $\boldsymbol{B}$, respectively. The result is a complete decomposition on the lefthand side, but a slightly interacting set on the righthand side. The first set is a modification of the traditional reaction invariant for a tank reactor, but affected by the reaction extent variables. True reaction invariance is not there. The interactions are caused by the transport properties of the various components and by heat. Only in the case of equal transport properties, that is, all diagonal elements in $\boldsymbol{T}$ are equal, will the conditions of true reaction invariance be achieved

$$\frac{d\xi}{dt} = [\boldsymbol{E}\boldsymbol{E}^T]^{-1} \boldsymbol{E}\boldsymbol{T}\boldsymbol{E}^T(\xi_0 - \xi) + [\boldsymbol{E}\boldsymbol{E}^T]^{-1} \boldsymbol{E}\boldsymbol{T}\boldsymbol{B}(\eta_0 - \eta) \tag{19}$$

If all elements in the diagonal matrix $\boldsymbol{T}$ are equal, that is, $\boldsymbol{T} = k\boldsymbol{I}$, then we will find that the condition that $\boldsymbol{E}\boldsymbol{T}\boldsymbol{B} = \boldsymbol{O}$ is true. This is the case with true reaction invariance. The surely stable reaction invariant vector ξ is then described by a set of uncoupled first-order differential equations

$$\frac{d\xi}{dt} = k(\xi_0 - \xi) \tag{20}$$

As in the stirred tank (Fjeld et al., 1974), the eigenvalues of Eq. 20 are all equal, $\lambda = -k$. The corresponding set of equations for the extents of reaction are from a premultiplication of Eq. 15 by $\boldsymbol{B}^T$

$$\frac{d\eta}{dt} = [\boldsymbol{B}^T\boldsymbol{B}]^{-1} \boldsymbol{B}^T \boldsymbol{T} \boldsymbol{E}^T(\xi_0 - \xi) + [\boldsymbol{B}^T\boldsymbol{B}]^{-1} \boldsymbol{B}^T \boldsymbol{T} \boldsymbol{B}(\eta_0 - \eta) + \boldsymbol{r} \tag{21}$$

Even here the decoupling is complete if all elements in the diagonal matrix $\boldsymbol{T}$ are the same, because then $\boldsymbol{B}^T\boldsymbol{T}\boldsymbol{E}^T = \boldsymbol{O}$. If this is not the case, the eigenvalues for the states ξ and η will be influenced by the individual transport properties.

Methanol Synthesis Reaction Kinetics

The above analysis may be applied to a practical reaction mechanism, first in the simplest form to judge whether catalyst particle stability represents a potential problem or not. For that purpose, a summary of the kinetic model for the methanol synthesis, as well as plausible transport properties, are presented here. The reaction rate models with their parameters are taken from Graaf et al. (1988). A later modification of the parameters corrected the experimental result for the interior transports in the particles (Graaf et al., 1990). Otherwise are catalyst data and reactor data proprietary.

Reaction mechanism

The reaction mechanism is suggested to comprise three reactions, the formation of methanol from carbon monoxide, the formation of methanol from carbon dioxide, and the water shift reaction

$$\text{Reaction No. 1} \quad -CO-2H_2+CH_3OH \leftrightarrow 0 \tag{22a}$$

$$\text{Reaction No. 2} \quad -H_2-CO_2+CO+H_2O \leftrightarrow 0 \tag{22b}$$

$$\text{Reaction No. 3} \quad -CO_2-3H_2+CH_3OH+H_2O \leftrightarrow 0 \tag{22c}$$

The rank of the stoichiometric matrix is 2, because the stoichiometry of the last reaction is the sum of that of reaction 1 and 2. Matrix $\boldsymbol{N}$ is rank deficient. From a stoichiometric point of view, and also from the point of view of heats of reaction, only two reactions are observable. The matrix $\boldsymbol{B}^T\boldsymbol{B}$ from Eq. 7b is singular, and its inverse does not exist. Hence, one reaction may be omitted. Let this reaction be the first reaction, where methanol is formed from carbon monoxide. This is in line with the latest observations of the reaction kinetics (Askgaard et al., 1995), where the significance of the first reaction is questioned. This leads to reduced matrices $\boldsymbol{N}$ and $\boldsymbol{B}$ for the methanol synthesis

$$\boldsymbol{N}''=\boldsymbol{N}\boldsymbol{R}''=\begin{bmatrix}1 & -1 & -1 & 1 & 0\\ 0 & -1 & -3 & 1 & 1\end{bmatrix} \tag{23a}$$

$$[\boldsymbol{B}'']^T=[\boldsymbol{B}\boldsymbol{R}'']^T=\begin{bmatrix}1 & -1 & -1 & 1 & 0 & \Delta T_{r,2}\\ 0 & -1 & -3 & 1 & 1 & \Delta T_{r,3}\end{bmatrix} \tag{23b}$$

Subscript r is reaction. In the atom matrix the first row represents carbon, the next hydrogen and the last oxygen. The first column represents carbon monoxide, the second carbon dioxide, the third hydrogen, the fourth water, and the fifth and last column represents methanol

$$\boldsymbol{A}=\begin{bmatrix}1 & 1 & 0 & 0 & 1\\ 0 & 0 & 2 & 2 & 4\\ 1 & 2 & 0 & 1 & 1\end{bmatrix} \tag{24a}$$

The extended atom matrix includes the heats of formation of the components, as shown in Eq. 7c

$$\boldsymbol{E}=\begin{bmatrix}1 & 1 & 0 & 0 & 1 & 0\\ 0 & 0 & 2 & 2 & 4 & 0\\ 1 & 2 & 0 & 1 & 1 & 0\\ -\Delta T_{f,1} & -\Delta T_{f,2} & 0 & -\Delta T_{f,4} & -\Delta T_{f,5} & 1\end{bmatrix} \tag{24b}$$

The material and heat balances of the reactions are uniquely described by the matrices $\boldsymbol{B}''$ and $\boldsymbol{E}$. Subscript f is formation.

Reaction rates

Extensive experimental investigations have been conducted by Graaf et al. for a copper catalyst (Graaf et al., 1988). The mechanism proposed by the authors has a rank deficient stoichiometric matrix, which indeed is a matter of concern for the parameter estimation in the reaction rates, as commented below. For convenience, the gas composition vector $\boldsymbol{c}$ in mole m^{-3} is defined as

$$c^T=[c_{CO},c_{CO_2},c_{H_2},c_{H_2O},c_{CH_3OH},c_{CH_4}] \tag{25}$$

The methane leakage is regarded as an inert in the reaction mechanism and in the reaction rates, but a high level of inert obviously slows down the reactions. Graaf et al. (1990) express the reaction rates as functions of temperature and the component fugacities $f_i=\varphi_i y_i P$ where y_i is the mole fraction, P the total pressure and φ_i the fugacity coefficient (subscripts i and j are the running index).

$$r_1=\frac{k_1K_1\left\{P^2\varphi_1y_1[\varphi_3y_3]^{3/2}-\dfrac{\varphi_5y_5}{[\varphi_3y_3]^{1/2}K_{p,1}}\right\}}{\{1+K_1P\varphi_1y_1+K_1P\varphi_1y_1\}\left\{[\varphi_3y_3]^{1/2}+\dfrac{K_4\varphi_4y_4}{[K_3P]^{1/2}}\right\}} \tag{26a}$$

$$r_2=\frac{k_2K_2P^{3/2}\left\{\varphi_2y_2\varphi_3y_3-\dfrac{\varphi_1y_1\varphi_4y_4}{K_{p,2}}\right\}}{\{1+K_1P\varphi_1y_1+K_1P\varphi_1y_1\}\left\{[\varphi_3y_3]^{1/2}+\dfrac{K_4\varphi_4y_4}{[K_3P]^{1/2}}\right\}} \tag{26b}$$

$$r_3=\frac{k_3K_3\left\{P^2\varphi_2y_2[\varphi_3y_3]^{3/2}-\dfrac{\varphi_5y_5\varphi_4y_4}{[\varphi_3y_3]^{3/2}K_{p,3}}\right\}}{\{1+K_1P\varphi_1y_1+K_1P\varphi_1y_1\}\left\{[\varphi_3y_3]^{1/2}+\dfrac{K_4\varphi_4y_4}{[K_3P]^{1/2}}\right\}} \tag{26c}$$

The coefficients are

$$k_i=\alpha_i\exp\left\{\frac{-E_i}{RT}\right\} \quad K_i=A_i\exp\left\{\frac{B_i}{RT}\right\}$$

$$\ln(K_{p,i})=-\frac{\Delta H_i^0-T\Delta S_i^0}{RT} \tag{26d}$$

R is a gas constant (J·mol^{-1}·K^{-1}). E_i is the activation energy of reaction No. i (J·mol^{-1}), k_i is the reaction kinetic rate constant (mol·kg^{-1}·bar$^{-1/2}$), and K_i is the adsorption equilibrium constant. $K_{p,i}$ is the reaction equilibrium constant, ΔS is the entropy change of formation (J·K^{-1}), and α_i is the frequency factor for reaction No. 1 (mol·kg^{-1}·s^{-1}·bar$^{-1/2}$). The fact that the stoichiometric matrix for the reactions in Eq. 22 has reduced rank indicates that there is a reduced set of basic reactions. This is indeed true, as shown in Eq. 23. If the first reaction is omitted as a basic reaction, two remaining basic reactions remain. Both the proposed kinetics (Graaf et al., 1988, 1990), the stoichiometry, and the heat balance are preserved by the reduced stoichiometric matrix in Eq. 23 and the reduced reaction rate vector

$$r'' = Rr = \begin{bmatrix} -1 & 1 & 0 \\ 1 & 0 & 1 \end{bmatrix} r \tag{27}$$

This result shows that the three-dimensional r is not observable from r'', which may raise a question to the adequacy and reliability of the parameter estimation in the article by Graaf et al. (1988, 1990).

The reaction rate r may also be related to the basic reaction rate r'' by

$$r = R''r'' = \begin{bmatrix} -1 & 1 \\ 0 & 1 \\ 1 & 0 \end{bmatrix} r'' \tag{28}$$

This implies that the product $RR'' = I$ is the identity matrix. Furthermore, the fact that the stoichiometry of the third reaction is the sum of the first two leads to the conclusion that the heat of reaction of the third reaction must be the sum of the heats of reaction of the other two. The heat of reaction of the reduced set may also be calculated from the heat of formation of the participating compounds

$$(-\Delta H_r'') = N''(-\Delta H_f'') \tag{29}$$

The relationship between the mole fraction vector y and concentration vector c on a volume basis may be estimated from the ideal gas law, because the fugacity coefficients are all very close to 1 at the operating pressure and temperature

$$y = \frac{RT}{P} c \tag{30}$$

Jacobian matrix of the reactor rate vector

The source of eventual instability is found in the reduced Jacobian matrix of the reaction rate, as quoted in Eq. 1. In the "bottom-up" system study of reactor stability, this phenomenon is studied first. The Jacobian is of dimension 2×2, as defined by the basic reaction rate r, the augmented state variable z, and the reduced stoichiometric matrix B''. According to Eq. 1, the Jacobian of the reaction rate vector may be written

$$J = \left[\frac{\partial r''}{\partial z}\right] B'' = \left[\frac{\partial r''}{\partial y}\frac{\partial y}{\partial c} \quad \frac{\partial r''}{\partial T} + \frac{\partial r''}{\partial y}\frac{\partial y}{\partial T}\right] B'' \tag{31}$$

The kinetic model developed by Graaf et al. (1988, 1990) has been used to evaluate the stability of the kinetics in a low pressure, industrial methanol reactor (Hansen, 1995). The spot tests of catalyst stability were taken at the inlet, at the temperature peak, and at the outlet. All eigenvalues were found to be negative, indicating full range stability, as shown in Table 1.

Table 1. Eigenvalues and Corresponding Time Constants at Various Locations for Jacobian to the Reaction Rate Vector

	Reactor Inlet	Temp. Peak	Reactor Outlet
Eigenvalues	−0.0717 −0.3358	−0.5501 −0.7918	−0.3412 −0.6125
Time constants, s	13.94 2.978	1.818 1.263	2.931 1.633

The kinetic response of the reactions, as indicated by the Jacobian matrix, is seen to increase with temperature. The time constants are smaller and the reactions are faster at higher temperatures. This is quite logical, as the Arrhenius terms make the reaction rates increase with temperature because all activation energies are positive. The fact that the eigenvalues are all negative shows that the catalyst particle is not likely to exhibit a runaway or an oscillating temperature history. Figures 2a–2c show how the eigenvalue location on

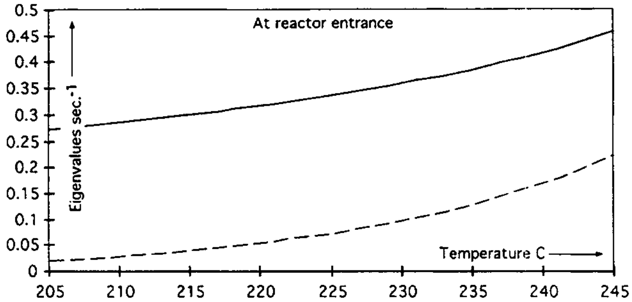

Figure 2a. Loci for negative real eigenvalues of the Jacobian matrix at reactor entrance.

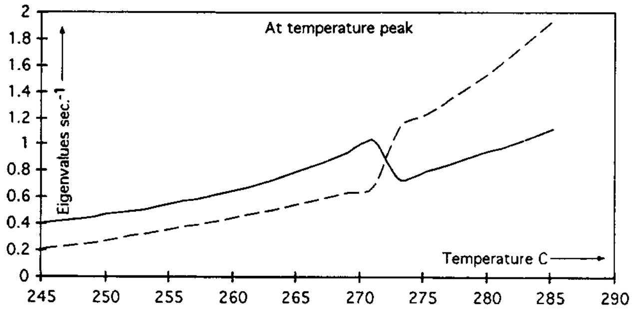

Figure 2b. Loci for negative real eigenvalues of the Jacobian matrix at temperature peak.

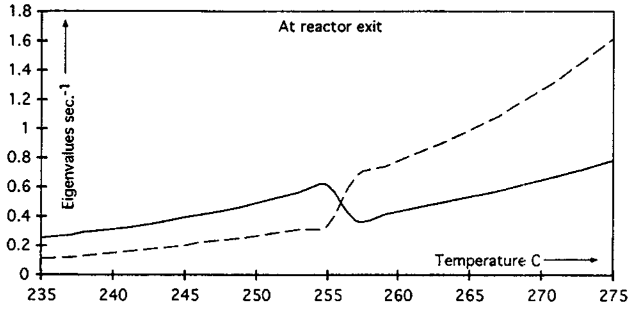

Figure 2c. Loci for negative real eigenvalues of the Jacobian matrix at reactor exit.

the negative real axis changes with temperature, equivalent to a root locus in the complex plane. Contrary to what might be believed, the eigenvalues move to the left as the temperature increases, that is, away from the right half plane, which means increased stability.

Increasing temperature moves the eigenvalues of the reaction matrix to the left in the negative half plane, hence increasing the stability in a "stirred tank" mode of operation, as the eigenvalues add to the space velocity, as shown in Eq. 1. Transport properties should have a similar stabilizing effect, as shown for the stirred tank. However, this effect needs to be evaluated.

An interesting observation is that there is a temperature down the reactor where the loci cross over. This means that the two eigenvalues are the same. This means that the radical is zero, while a negative radical will cause damped oscillations. However, such oscillations will not occur in the commercial reactor and the conclusion so far indicates a smooth and stable operation of the reactor, as far as the catalyst is concerned.

External transport properties

The driving force in Eq. 11 is a difference in molar concentration on a mass basis. A simple model on a mole fraction basis may be used for the estimation of mass-transfer rate from the bulk of the gas into the particle (Graaf et al., 1990)

$$k_i = \frac{a_m u_g}{Re^{b_m} Sc_i^{2/3}} \qquad Re = \frac{w d_p}{\mu_g} \qquad Sc_i = \frac{\mu_g}{\rho_g D_i} \tag{32}$$

a_m is a mass-transfer coefficient parameter, and b_m is the Reynolds number (Re) exponent in the mass-transfer coefficient. Sc is the Schmidt number, w is the mass flux ($kg \cdot m^{-2} \cdot s^{-1}$), and μ is the viscosity ($kg \cdot s^{-1} \cdot m^{-1}$). According to Graaf et al. (1988, 1990), the effective component diffusivity in the particle is inversely proportional to the square root of the molecular weight, and may be estimated to

$$D_i = \frac{4\epsilon_p a_p}{3\tau_p}\sqrt{\left[\frac{2RT}{\pi M_i}\right]} \tag{33}$$

a_p is the average catalyst pore diameter, m. M_i is the mole weight for component i ($kg \cdot mol^{-1}$). This diffusivity may be used in the boundary layer near the particle surface, that is, Eq. 32. The only variation in the diffusivity from one component to the next, is the mole weight; the diffusivity increases with the inverse cubic root of the mole weight. The effect of temperature is common to all components, the diffusivities increase with the cubic root of the temperature.

The effects of the external transport phenomena on the particle dynamics may be included in the pellet model by the matrix $\boldsymbol{T}$ in Eq. 15 and the characteristic matrix in Eqs. 19 and 21. The calculations have been performed for typical transport data and operating conditions for an industrial reactor, and summarized in Table 2. The eigenvalues again show complete stability at the inlet, at the temperature peak, and at the outlet as shown in Table 2.

Table 2. Eigenvalues and Corresponding Time Constants Imposed by External Transport Phenomena

Eigenvalues, s^{-1}			Time Constants, s		
Reactor Inlet	Temp. Peak	Reactor Outlet	Reactor Inlet	Temp. Peak	Reactor Outlet
−96.337	−100.616	−97.207	0.01038	0.00994	0.01029
−46.704	−48.706	−47.064	0.02141	0.02053	0.02125
−40.136	−42.272	−40.794	0.02492	0.02366	0.02451
−38.334	−39.958	−38.641	0.02609	0.02503	0.02588
−34.539	−36.259	−34.936	0.02895	0.02758	0.02862
−0.76058	−0.76100	−0.76066	1.31479	1.31406	1.31464

When the entries in Table 2 are compared with those in Table 1, a marked difference in the speed of response is noticed. The particle response is now much faster with time constants close to a second. Since the resulting eigenvalues may be regarded as a superposition of those from the transport phenomena and those from the kinetics, the result shows that the particle takes the bulk gas conditions very rapidly. The transport properties bring the particle states very close to equilibrium conditions with the bulk gas states. This is indeed observed in the modeling of the methanol reactor (Hillestad, 1995). Another important observation is that the eigenvalues are less dependent on the position in the reactor, which is also quite obvious because the dominance from the reaction kinetics is practically eliminated. One time constant is significantly greater than the others, which is ascribed physically to the temperature dynamics. The particle heat accumulation capacity contributes to a much slower response than the mass accumulation capacity. The variations in the other eigenvalues stem from the variation in individual mass-transfer coefficients by the mole weight differences. Furthermore, the slight variation in eigenvalues with reactor operation stems from the temperature dependence of the transport properties.

An important question to be posed after these observations is how the internal transport phenomena affect the catalyst particle dynamics. The simplest approach divides the spherical particle into equal volume shells as a difference approach to the partial differential equation of material and heat balance.

Internal transport properties

The transport phenomena inside the porous catalyst particle are governed by the molecular and the Knudsen diffusion for the individual components. The convective transport is neglected as supported by orders of magnitude evaluations. The reaction invariance is destroyed by internal transport phenomena as well. The kinetic rate expression is a source term in the material balance described by a partial differential equation for the interior of the particle. Let the dimensionless spherical coordinate be $x = d/d_p$. Then

$$\frac{\partial z}{\partial t} = \frac{4D}{d_p^2}\left(\frac{2}{x}\frac{\partial z}{\partial x} + \frac{\partial^2 z}{\partial x^2}\right) + Br \tag{34}$$

t is time (s). The decomposition in Eqs. 19 and 21 is still valid for this equation, but the different diffusivities introduce an interaction between the apparent reaction invariant and the extent of reaction

$$\frac{\partial \xi}{\partial t}=\frac{4[EE^T]^{-1}}{d_p^2}\left\{EDE^T\left(\frac{2}{x}\frac{\partial \xi}{\partial x}+\frac{\partial^2 \xi}{\partial x^2}\right)+EDB\left(\frac{2}{x}\frac{\partial \eta}{\partial x}+\frac{\partial^2 \eta}{\partial x^2}\right)\right\} \quad (35a)$$

and

$$\frac{\partial \eta}{\partial t}=4[B^TB]^{-1}\left\{B^TDE\left(\frac{2}{x}\frac{\partial \xi}{\partial x}+\frac{\partial^2 \xi}{\partial x^2}\right)+B^TDB\left(\frac{2}{x}\frac{\partial \eta}{\partial x}+\frac{\partial^2 \eta}{\partial x^2}\right)\right\}+r \quad (35b)$$

The interaction between the dynamic modes are again seen to be caused by the matrix D. If this is approximated by $\mathfrak{D}I$, then the reaction invariants will proceed through the pellet as a purely physical diffusion phenomenon, as if the reactions did not occur. $\mathfrak{D}$ is the diagonal matrix of component diffusivities ($m^2 \cdot s^{-1}$).

A rough estimate of the effect of internal transport phenomena may be obtained by a simple lumped stagewise model. The catalyst particle volume is divided into equal halves. The ratio between the radius of the inner core and the particle outer radius is then the cubical root of 0.5. The transport from the bulk to the outer shell corresponds to the matrix K, and the transport between the outer shell and the inner core is described by a simple discretization of Eq. 35

$$\frac{dz_1}{dt}=a_k K(z_g-z_1)-a_d D(z_1-z_2)+Br(z_1)$$

$$a_k=2 \qquad a_d=\frac{24}{(1-\sqrt[3]{0.5})\epsilon d_p^2} \quad (36a)$$

$$\frac{dz_2}{dt}=a_d D(z_1-z_2)+Br(z_2) \quad (36b)$$

As before, the kinetic matrix appears along the diagonal of this extended matrix, while the transport properties appear along the diagonal and the two side-traces. For a given set of reactor conditions, a summary of the eigenvalues is given in Table 3.

The same pattern in the distribution of the eigenvalues, as in Table 2, is indeed observed in Table 3. The five first large ones are associated with the mass transfer and mass accumulation in the outer shell of the particle. The sixth eigenvalue is associated with the heat accumulation dynamics of the outer shell, which now has only one-half the capacity, as shown in Table 2. Consequently, the eigenvalue is about twice as big. The following six eigenvalues are associated with the inner core of the particle. This shows much smaller eigenvalues, due to the transport limitation by Knudsen diffusion and heat conduction in the particle. The results in Tables 2 and 3 make physical sense, and satisfy the industrial requirements to this investigation. A further development of the model into a fully distributed variable model, as in Eq. 35, is not justified. The practical conclusion is that the likelihood for temperature oscillations in the methanol catalyst particles is indeed very small, if not nonexistent.

Table 3. Effect of Internal Transport Phenomena on Catalyst Particle Stability

Eigenvalues, s^{-1}			Time Constants, s		
Reactor Inlet	Temp. Peak	Reactor Outlet	Reactor Inlet	Temp. Peak	Reactor Outlet
−56.847	−59.448	−57.436	0.0176	0.0168	0.0174
−27.654	−28.844	−27.879	0.0362	0.0347	0.0359
−23.696	−25.154	−24.243	0.0422	0.0398	0.0413
−22.614	−23.570	−22.809	0.0442	0.0424	0.0438
−20.394	−21.501	−20.686	0.0490	0.0465	0.0483
−1.5419	−1.7970	−1.6841	0.6486	0.5565	0.5938
−0.9571	−1.6519	−1.2386	1.0448	0.6486	0.8073
−0.8767	−0.9576	−0.9572	1.1407	1.0443	1.0447
−0.6832	−0.9409	−0.8808	1.4637	1.0628	1.1354
−0.5964	−0.6470	−0.6137	1.6767	1.5455	1.6294
−0.5517	−0.6200	−0.6123	1.8126	1.6129	1.6332
−0.1296	−0.1298	−0.1297	7.7144	7.7045	7.7108

The computer simulations presented as results in Tables 1 through 3 have been realized in a MATLAB programming system (The MathWorks, 1992, 1993), which is extremely useful for rapid prototyping of program systems with involved mathematics. This is a thoroughly tested and reliable package, leaving no doubts as to the correctness of the eigenvalue calculations.

Conclusion

It is shown that different rates of component and heat transport between a bulk fluid and a catalyst particle destroy the reaction invariant phenomena applied to flow reactors such as stirred tanks and tubular flow reactors. This also affects the stability conditions for the particle, which cannot be treated like a "stirred tank" approximation, even if the internal gradients of temperature and concentration are negligible. To what extent this is significant in an industrial operation depends upon reaction rates transport coefficients and so on. Quantitative evaluations are only possible with concrete cases, which is demonstrated by the methanol synthesis catalyst particle at typical operating conditions in an industrial reactor. The roots to instability for a catalyst particle are found in the Jacobian matrix to the primary, independent reaction rates, and a systematic evaluation of catalyst stability locally starts with the eigenvalues to this matrix. Some interesting properties of the root loci, such as a crossing over, are found when the eigenvalues are plotted vs. temperature for the methanol kinetics.

From a simple two-stage model, it is shown that the speed of response of the inner core of the particle is much slower than the outer shell, even if the temperature profile throughout the particle is shown to be fairly constant. It is also shown that the particle has thermal stability at all practical operating conditions throughout an industrial reactor. Another conclusion that can be drawn from the investigation is that the internal resistance to mass transport inside the particle is significant, while the resistance to heat conduction in the particle is negligible. The reason why the speed of response of temperature is almost a decade slower than the speed of concentration response is found in the vast difference in accumulation capacity, and not in the transport resistance.

The physical interpretation of the stability analysis makes perfect sense, and it is felt that the dynamics of the catalyst are well understood. It is possible to observe a significant resistance to transport, and still a faster speed of dynamic response, if the accumulation capacity is small enough. This is exactly what is observed as the fundamental difference between the mass and heat transport to and inside the catalyst particle. The observed order of magnitude of the speed of response and the potential differences in the driving force helps to understand the operating conditions for the catalyst particle when in reactor operation.

Acknowledgment

The authors express their appreciation to the Statoil Company for their support in carrying out this investigation and their subsequent permission to publish the results. For understandable reasons, there are data behind the numerical calculations that cannot be revealed. Thanks are also due to the SKARPODD Company which has provided programming assistance and computer facilities.

Literature Cited

Aris, R., "On Stability Criteria of Chemical Reaction Engineering," *Chem. Eng. Sci.*, **24**, 149 (1969).

Asbjornsen, O. A., "The Distribution of Residence Times in a Falling Water Film," *Chem. Eng. Sci.*, **14**, 211 (1960).

Asbjornsen, O. A., "The Distribution of Residence Times in a Falling Water Film," Doctor Technicae Diss., Norwegian Technical Univ. (1962).

Asbjornsen, O. A., "Reaction Invariance in Chemical Reactor Dynamics," *Kemian Teolisuus*, 10, 633 (1972).

Asbjornsen, O. A., *Process Dynamics*, Tapir Printing Press, Trondheim, Norway (1974).

Asbjornsen, O. A., "Modeling Techniques: Theory and Practice," *Modeling, Identification and Control*, **6**(3), 105 (1985).

Asbjornsen, O. A., "Chemical Reactor Control," *Systems and Control Encyclopedia*, Madan G. Singh, ed., Vol. I, Pergamon Press, Oxford, p. 585 (1987a).

Asbjornsen, O. A., "A Systems Engineering Approach to Process Modeling," *Shell Workshop on Process Control*, D. M. Prett and M. Morari, eds., Butterworth Pub., p. 139 (1987b).

Asbjornsen, O. A., "Electrolysis Control," *Systems and Control Encyclopedia*, Madan G. Singh, ed., Vol. II, Pergamon Press, Oxford, p. 1413 (1987c).

Asbjornsen, O. A., "Chemical Reactor Modeling," *Concise Encyclopedia of Modeling and Simulation*, M. G. Singh, D. P. Atherton, and P. Borne, eds., Pergamon Press, Oxford, p. 50 (1992).

Asbjornsen, O. A., and M. Fjeld, "Response Modes of a Continuous Stirred Tank Reactor," *Chem. Eng. Sci.*, **25**, 1627 (1970).

Askgaard, T. S., J. K. Nørskov, C. V. Ovesen, and P. Stoltze, "A Kinetic Model of Methanol Synthesis," *J. of Catal.*, **156**, 229 (1995).

Åström, K. J., and B. Wittenmark, *Computer Controlled Systems*, Prentice-Hall, Englewood Cliffs, NJ (1984).

Balakotaiah, V., and D. Luss, "Explicit Runaway Criterion for Catalytic Reactors with Transport Limitations," *AIChE J.*, **37**, 1780 (1991).

Bird, R. B., W. E. Stewart, and E. N. Lightfoot, *Transport Phenomena*, Wiley, New York (1960).

Denbigh, K., *The Principles of Chemical Equilibrium*, Cambridge, The Univ. Press, Cambridge, England (1964).

Fjeld, M., O. A. Asbjornsen, and K. J. Åström, "Reaction Invariance and Their Importance in the Analysis of Eigenvectors, State Observability and Controllability of the Continuous Stirred Tank Reactor," *Chem. Eng. Sci.*, **29**, 1917 (1974).

Glasstone, S., and D. Lewis, *Elements of Physical Chemistry*, Macmillan, London (1964).

Graaf, G. H., H. Scholtens, E. J. Stamhuis, and A. A. C. M. Beenackers, "Intra-Particle Diffusion Limitations in Low-Pressure Methanol Synthesis," *Chem. Eng. Sci.*, **45**, 773 (1990).

Graaf, G. H., E. J. Stamhuis, and A. A. C. M. Beenackers, "Kinetics of Low-Pressure Methanol Synthesis," *Chem. Eng. Sci.*, **43**, 3185 (1988).

Hansen, R., Personal Communications, *Statoil as* (1995).

Hillestad, M., "Fixed Bed Reactor Modeling—Methanol Synthesis," *Internal Statoil Report*, NED95189 (in Norwegian) (1995).

Hu, R., V. Balakotaiah, and D. Luss, "Multiplicity Features of Catalytic Pellets: III. Uniqueness Criteria for the Lumped Thermal Model," *Chem. Eng. Sci.*, **41**, 1525 (1986).

Hugo, P., "Zum dynamischen Verhalten stark exothermer katalytischer Reaktionen im offenen Kreislauf," *Chemical Reaction Engineering*, Pergamon Press Ltd., Oxford, p. 459 (1971).

Lewis, G. N., and M. Randall, *Thermodynamics*, 2nd ed., McGraw-Hill, New York (1961).

MATLAB Reference Guide, The MathWorks, Inc., Natick, MA (1992).

MATLAB User's Guide, The MathWorks, Inc., Natick, MA (1993).

Philippou, G., M. Somani, and D. Luss, "Traveling Temperature Fronts on Catalytic Ribbons," *Chem. Eng. Sci.*, **48**, 2325 (1993).

Wicke, E. G., Padberg, and H. Arens, "Instabilitäten bei exothermen katalytischer Gasreaktionen in adiabatischer Kontaktschicht," *Chemical Reaction Engineering*, Pergamon Press, Oxford, p. 425 (1971).

Manuscript received May 24, 1995, and revision received Oct. 15, 1996.